Biochimica et Biophysica Acta 1798 (2010) 515–525

Contents lists available at ScienceDirect

Biochimica et Biophysica Acta

journal homepage: www.elsevier.com/locate/bbamem

P-glycoprotein substrate transport assessed by comparing cellular and vesicular ATPase activity

Pierluigi Nervi, Xiaochun Li-Blatter, Päivi Äänismaa, Anna Seelig *

Biophysical Chemistry, Biozentrum, University of Basel, Klingelbergstrasse 70, Switzerland

ARTICLE INFO

Article history:
Received 28 August 2009
Received in revised form 13 November 2009
Accepted 26 November 2009
Available online 14 January 2010

Keywords:
ATPase activity
Extracellular acidification rate
Passive diffusion
Influx
P-glycoprotein substrate
Active efflux

ABSTRACT

We compared the P-glycoprotein ATPase activity in inside–out plasma membrane vesicles and living NIH-MDR1-G185 cells with the aim to detect substrate transport. To this purpose we used six substrates which differ significantly in their passive influx through the plasma membrane. In cells, the cytosolic membrane leaflet harboring the substrate binding site of P-glycoprotein has to be approached by passive diffusion through the lipid membrane, whereas in inside–out plasma membrane vesicles, it is accessible directly from the aqueous phase. Compounds exhibiting fast passive influx compared to active efflux by P-glycoprotein induced similar ATPase activity profiles in cells and inside–out plasma membrane vesicles, because their concentrations in the cytosolic leaflets were similar. Compounds exhibiting similar influx as efflux induced in contrast different ATPase activity profiles in cells and inside–out vesicles. Their concentration was significantly lower in the cytosolic leaflet of cells than in the cytosolic leaflet of inside-out membrane vesicles, indicating that P-glycoprotein could cope with passive influx. P-glycoprotein thus transported all compounds at a rate proportional to ATP hydrolysis (i.e. all compounds were substrates). However, it prevented substrate entry into the cytosol only if passive influx of substrates across the lipid bilayer was in a similar range as active efflux.

1. Introduction

The ATP binding cassette transporter (ABC) P-glycoprotein (Pgp, MDR1, ABCB1) is present in the plasma membrane of most cells. Especially high expression levels are found in the apical membranes of epithelial cells that play a role in absorption of exogenous compounds (e.g. blood–brain barrier and intestinal barrier) or excretion of metabolites (e.g. liver and kidney). The expression level is also high in many tumor cells where Pgp contributes to multidrug resistance, MDR (for review see [1]). It is known that Pgp binds its substrates in the cytosolic membrane leaflet of apical membranes [2,3] and flips them back to the outer leaflet at the expense of ATP hydrolysis [4]. A direct correlation between substrates transported and ATP molecules hydrolyzed in inside–out plasma membrane vesicles or proteoliposomes has long been suggested [5–7]. However, this correlation is rather difficult to prove experimentally, since Pgp substrates are generally electrically neutral or cationic (with intermediate or low ionization constants, i.e. $pK_a<9$) and strongly accumulate in the lipid membrane. If they are moreover small they diffuse rapidly through the lipid membrane and escape partially to the cytosol before being caught by Pgp in the cytosolic membrane leaflet, a phenomenon low. Dubbed the pump-leak mechanism by Stein [8] (see also (e.g. [9,10]). Using spin labeled verapamil which carries a quaternary ammonium ion and therefore cannot cross the lipid bilayer by passive diffusion the correlation between ATPase activity and transport was demonstrated convincingly [11]).

The direct correlation between Pgp ATPase activity and transport was further demonstrated by assessing the net flux of drugs across a single membrane as the sum of active efflux by Pgp, V, (i.e. ATPase activity) and passive influx, Φ_M, across the lipid bilayer. To this purpose active efflux across the plasma membrane of NIH-MDR1-G185 cells was measured and passive influx, Φ_M, across the lipid bilayer was quantitatively estimated based on Fick's law, taking into account the cross-sectional area of the diffusing molecule in its membrane-bound conformation and the lateral packing density of the lipid bilayer. The analysis revealed that compounds diffusing rapidly across the cell membrane reach the cytosol despite being transported by Pgp, whereas compounds diffusing slowly do not reach the cytosol because Pgp can cope with their influx. The latter compounds corresponded to those which are considered as transported in bi-directional transport assays [12,13].

Bi-directional transport assays are most commonly used to investigate substrate transport by Pgp (see e.g. [14–16]). To this purpose, polarized epithelial cells (e.g. MDCK or LLC-PK cells) are cultured on a filter insert that separates an apical and a basolateral compartment. This setup allows measurement of the net flux of compounds from the basolateral-to-apical and the apical-to-basolateral side of confluent cell monolayers. If the flux of compounds in the

Abbreviations: ABC, ATP binding cassette transporter; ATP, adenosine triphosphate; ECAR, extracellular acidification rate; MDR, multidrug resistance; Pgp, human P-glycoprotein-ATPase (MDR1, ABCB1)

* Corresponding author. Tel.: +41 61 267 22 06; fax: +41 61 267 21 89.
E-mail address: Anna.Seelig@unibas.ch (A. Seelig).

0005-2736/$ – see front matter © 2009 Elsevier B.V. All rights reserved.
doi:10.1016/j.bbamem.2009.11.022

basolateral-to-apical direction is higher than in the opposite direction, efflux transporters are likely to be involved. The flux from the basolateral-to-apical side includes passive flux across the entire cell, Φ_C, plus active export across the apical membrane, V, $(\Phi_C + V)$, and the flux from the apical-to-basolateral side includes passive flux across the entire cell, Φ_C, minus active transport across the apical membrane, V, $(\Phi_C - V)$, whereby the flux Φ_C is the product of the permeability coefficient, P, and the concentration gradient, ΔC (e.g. [13]). Compounds with a positive flux ratio $(r = (\Phi_C + V) / (\Phi_C - V) > 1)$ are conventionally defined as "substrates". A positive flux ratio in the order of $r \approx 1.2$ to 11 is obtained if the passive flux, Φ_C, is ~10 to ~1.2-fold faster than active efflux, V. Neither compounds exhibiting higher passive influx (more than 10 times higher than active efflux) nor compounds exhibiting a lower passive influx than efflux are recognized as "substrates", even though they may be transported by Pgp. Passive influx, Φ_C, across the cell layer is generally assessed by blocking Pgp with inhibitors such as verapamil or GF-120918 (see e.g. [17]) that are cationic. At the high concentrations required for Pgp inhibition, the compounds partition strongly into the lipid bilayer and tend to impart a positive surface potential to the plasma membrane [18], which in turn leads to reduced partitioning of further cationic substrates. Passive influx, Φ_C, estimated by inhibiting Pgp in bi-directional transport assays is therefore generally too low. A quantitative interpretation of transport data at the molecular level is complicated by the fact that drugs have to cross the entire cell layer, and separation of active efflux, V, and passive influx, Φ_C, is difficult.

The aim of the present study was to investigate transport across a single membrane and to experimentally test the relation between passive compound influx, Φ_M, and apparent compound efflux, V, by Pgp. In cells, the cytosolic leaflet of the plasma membrane which harbors the substrate binding site of Pgp has to be approached by passive diffusion across the lipid bilayer, whereas in inside–out plasma membrane vesicles it is accessible directly from the aqueous phase. If passive influx, Φ_M, from the extracellular to the cytosolic membrane leaflet is fast compared to active efflux, V, by Pgp, the drug concentration in the cytosolic membrane leaflet should be similar in cells and inside–out plasma membrane vesicles. Under these conditions the ATPase activity, V, which directly reflects the drug concentration in the cytosolic membrane leaflet [19] should also be similar, as was indeed observed previously [20,21]. However, if passive influx, Φ_M, across the membrane approaches active efflux, V, by Pgp, the drug concentration in the cytosolic membrane leaflet should be lower in cells than in inside–out membrane vesicles and the Pgp ATPase activity profiles should no longer be identical. To test this assumption, we measured the Pgp ATPase activity in cells and in inside–out plasma membrane vesicles under steady-state conditions by monitoring the substrate-induced extracellular acidification rate, ECAR, [21] and phosphate release rate [20], respectively. As compounds we used three cationic drugs (verapamil, diltiazem and daunorubicin) and three electrically neutral detergents ($C_{12}EO_8$, Triton X-100 and Tween 80). The drugs [21] and the detergents [22] all bind to Pgp but differ significantly in their passive influx, Φ_M, through the plasma membrane at their concentration of half-maximum Pgp activity, K_1. Passive influx, Φ_M, across the lipid bilayer of the plasma membrane was quantitatively estimated based on Fick's law, using the data from surface activity measurements as described previously [13].

The comparison of the ATPase activity in cells and inside–out plasma membrane vesicles revealed that Pgp can establish a concentration gradient between the cytosolic and extracellular plasma membrane leaflet in cells (with a higher concentration in the cytosolic leaflet) if passive substrate influx, Φ_M, approaches active substrate efflux, V. However, no concentration gradient can be established, despite the fact that the compounds are transported by Pgp, if influx is significantly higher than efflux. The comparison of ATPase activity profiles in cells, where diffusion occurs prior to binding, and inside–out membrane vesicles, where no diffusion step is required, thus allows fast and convenient assessment of apparent substrate transport by Pgp which neither system alone could provide.

2. Materials and methods

2.1. Compounds

The nonionic detergents $C_{12}EO_8$ (dodecyloctaglycerol), Triton X-100, Tween 80 (polysorbate-80) and the cationic drugs daunorubicin·HCl, diltiazem·HCl, (R/S)-verapamil·HCl were purchased from Sigma-Aldrich (St. Louis, MO, USA).

2.2. Cell lines and cell culture

Mouse embryo fibroblasts stably transfected with the human *MDR1* gene (NIH-MDR1-G185) [23] and the corresponding wild-type cells (NIH-3T3) were a kind gift from Dr. M.M. Gottesman (National Cancer Institute, Bethesda, U.S.A.). Cells were grown as monolayer cultures in sterile cell culture flasks (Costar, 25–75 cm^2) and were incubated at 37 °C in a Heraeus Incubator in an air atmosphere supplemented with 5% CO_2 and humidity saturation of 100%. As cell culture medium, DMEM (containing 4.5 g/L glucose) was chosen, supplemented with 1% L-glutamine (146 mg/L), streptomycin (100 μg/mL), penicillin (100 U/mL) and 10% FBS (v/v). NIH-MDR1-G185 cells were kept under growth selection with 0.15 μM (60 ng/mL) colchicine. Passages (1:10) and (1:20) for NIH-MDR1-G185 and NIH-3T3 cells, respectively, were performed twice a week, from confluent cultures, after treatment with trypsin–EDTA (Gibco). Cellular stock aliquots of 10^7 cells/mL were prepared in DMEM, 10% DMSO, 10% FBS and were kept in 1.8 mL *Nunc CryoTubes* frozen in liquid nitrogen.

NIH-MDR1-G185 cells were characterized by means of FACS analysis using the monoclonal, Pgp-specific antibody MRK16 and a second fluorescent FITC-labeled antibody. No wild-type contamination was observed [24]. The good agreement between the vinblastine- and verapamil-stimulated Pgp ATPase activities measured by Ambudkar et al. [6] and Aanismaa et al. [20] suggested that the expression level of Pgp in NIH-MDR1-G185 cells has remained approximately constant over time.

2.3. Cytosensor measurements

Extracellular acidification rates, ECARs, were monitored in real time using an eight-channel Cytosensor® Microphysiometer (Molecular Devices, Menlo Park, CA, U.S.A.) [25]. This device is based on silicon technology and allows detection of pH changes down to 0.001 pH U/min by means of a light addressable potentiometric sensor, LAPS. Protons excreted by cells upon stimulation come into contact with the LAPS and induce a change in the applied voltage in the order of a few μVolts s^{-1}. According to the calibration, 61.0 ± 1.1 mV corresponds to 1 pH unit. The calibration of the instrument is discussed in detail elsewhere [24].

Aliquots of $(3–4) \times 10^5$ cells were seeded into capsule cups (12-mm-diameter plates with a microporous polycarbonate membrane bottom) and were left in the incubator overnight for sedimentation in the presence of the same medium used for culture, however, without colchicine. For Cytosensor measurements, capsule cups were transferred into the sensor chambers, adequately covered with capsule spacers and inserts, in order to create a tight chamber of 2.8 μL. Thus, the actual number of cells available for the measurement was reduced to ~1/4 of the total amount. The system was stabilized at 37 °C and cells were superfused with DMEM without sodium bicarbonate to limit pH buffering (100 μL/min). In order to preserve the osmotic balance the lacking sodium bicarbonate was replaced by sodium chloride (2.6 g/L NaCl instead of 3.7 g/L $NaHCO_3$) in the case

of drugs. In the case of detergents, sodium chloride was omitted. The flow medium was supplemented with 1 mM sodium pyruvate to decrease the basal ECAR and to enhance the relative ECAR changes due to Pgp activation [24].

The peristaltic pumps were programmed to function for 1 min 40 s, and then to stop for a period of 20 s, in a periodic cycle. During the 20-s pause interval, acidic metabolites accumulated in the sensor chamber. The ECAR recorded in $\mu V\ s^{-1}$, started 5 s after pump stop and lasted for 13 s. All data were directly processed by the software Cytosoft for Macintosh (Molecular Devices, Menlo Park, CA, U.S.A.). Before Pgp stimulation, cells were allowed to reach a stable ECAR (30 min to 1 h). For stimulations, the normal running medium was switched to the drug containing medium for 3 min. During this period, two ECAR data points were recorded, one after 40 s (transient situation) and the second 2 min later (steady-state conditions established). For data analysis, the cellular ECAR change corresponding to the second point was considered, normalized to the basal activity, and therefore expressed in percentage of the basal ECAR taken as 100%. The substrate concentration reaching the measuring cell was corrected for adsorption to the Cytosensor tubing in the case of drugs by means of spectroscopic measurements. An analogous correction is not possible in the case of detergents. For details see [21].

2.4. Plasma membrane preparation and ATPase measurements

The inside–out plasma vesicles were prepared as described in detail elsewhere and exhibited a predominant inside–out orientation [20]. The vesicles showed a rather broad size distribution with an average diameter of approximately 1000 nm as determined with a Zetasizer Nano, ZS. Due to the large diameter the lateral membrane packing density in vesicles can be assumed to correspond approximately to that in cells. The ATPase activity was monitored by means of a colorimetric phosphate release assay as described in detail elsewhere [20]. Measurements were performed at pH 7.4 whereas previous measurements were performed at pH 7.0.

2.5. Kinetic data evaluation

The Pgp ATPase activity measured as a function of the substrate concentration generally yields bell-shaped profiles which are best interpreted in terms of two-site binding models [26,27]. The model proposed by Al-Shawi et al. [27] is based on non-competitive inhibition and assumes that the transporter is blocked if the second site is occupied, whereas the model proposed by Litman et al. [26] is based on un-competitive or substrate inhibition and allows for transport, although, at a reduced rate, even if the second binding site is occupied (for details see [21]). Recent competition experiments [22] support the latter model and suggest that the two binding sites are juxtaposed [21,22].

We fitted the bell-shaped activity curves with Eq. (1) [26]. The model assumes transporter activation, if one substrate molecule is bound to the transporter and inhibition if a second substrate molecule is bound to the transporter as described by the following equation,

$$V_s = \frac{K_1K_2V_0 + K_2V_1C_S + V_2C_S^2}{K_1K_2 + K_2C_S + C_S^2} \quad (1)$$

where V_0 is the basal activity in the absence of substrates, V_1 is the maximum transporter activity (if only activation occurred), V_2 is the activity at infinite substrate concentration, and C_S is the substrate concentration in aqueous solution. The kinetic parameters can be obtained either by titrating Pgp with substrates in living cells or inside–out plasma membrane vesicles, by monitoring the rate of lactate release (i.e. ECAR) [21] or the rate of P_i release [20], respectively.

2.6. Surface activity measurements

Surface activity measurements were performed at room temperature with the Wilhelmy vertical plate method, as described in detail elsewhere [28,29]. Stock solutions were prepared in pure water and serial aliquots were injected by means of a Hamilton syringe into a 20- or 3 -mL Teflon trough filled with buffer (50 mM Tris/HCl, containing 114 mM NaCl, pH 7.4 or pH 8.0) and the surface pressure, π, was monitored as a function of time until equilibrium (i.e. a constant surface pressure) was reached.

The thermodynamics of drug absorption at the air–water interface is described by the Gibbs adsorption isotherm

$$d\pi = RT\Gamma d\ln C, \quad (2)$$

where π is the surface pressure, RT is the product of the gas constant and the absolute temperature, C is the concentration of the amphiphile in bulk solution in the monolayer trough and Γ is the surface excess concentration of the amphiphile at the air–water interface. The surface excess concentration can be expressed as

$$\Gamma = (N_A A_S)^{-1} \quad (3)$$

where N_A is the Avogadro number and A_S the area requirement of the molecule at the air–water interface. The surface excess concentration, Γ, increases with increasing concentration up to a limiting value Γ_∞. The limiting value Γ_∞ was determined from the quasi-linear part of the Gibbs adsorption isotherm,

$$\Gamma_\infty = (1/RT)d\pi / d\ln C. \quad (4)$$

Knowledge of the limiting surface concentration, Γ_∞, allows estimation of the limiting cross-sectional area of the molecule, A_D, in its amphiphilic orientation at the air–water interface (see Eq. (2)). In the case of cationic drugs, the Gibbs adsorption isotherms were also measured at pH 8.0 to minimize the charge repulsion effects and to obtain the effective molecular cross-sectional area, A_D, [30]. It can be assumed that molecules inserted into the lipid–water interface adopt the same amphiphilic orientation as in the air–water interface and thus exhibit a similar cross-sectional area, A_D, [31].

To evaluate the air–water partition coefficient, K_{aw}, the Szyszkowski equation,

$$\pi = RT\Gamma_\infty \ln(K_{aw}C + 1) \quad (5)$$

was used. The concentration, C, corresponds to the equilibrium concentration of the drug, C_{eq}, in bulk solution that is defined as the total concentration, C_{tot}, minus the concentration of the drug adsorbed to the air–water interface, C_b, [29]

$$C_{eq} = C_{tot} - C_b. \quad (6)$$

The concentration, C_b, is the product of the surface excess concentration, Γ, and the surface area, A, per total volume, V of the solution in the trough ($C_b = \Gamma_\infty(A/V)$). For small and intermediate air–water partition coefficients ($K_{aw} < 10^6\ M^{-1}$), the concentration adsorbed to the air–water interface, C_b, is negligibly small ($C_{eq} \sim C_{tot}$). In the present investigation, we corrected for the concentration, C_b, since detergents exhibit rather large air–water partition coefficients, K_{aw}.

2.7. Estimation of lipid–water partition coefficients

The lipid–water partition coefficient, K_{lw}, defined as

$$K_{lw} = X_b / C_{eq}, \quad (7)$$

where X_b is the mole fraction of drug bound to the membrane and C_L is the lipid concentration.

$$X_b = C_b / C_L. \quad (8)$$

The lipid–water partition coefficient, K_{lw}, can be derived from the air–water partition coefficient, K_{aw}, if the cross-sectional area, A_D, of the drug and the lateral lipid packing density of the membrane, π_M, are known [30]

$$K_{lw} = K_{aw} \cdot e^{-\pi_M A_D / kT}, \quad (9)$$

where k is the Boltzmann constant and T the absolute temperature. If the lipid membrane exhibits a surface potential, ψ, Eq. (9) can be modified

$$K_{lw} = K_{aw} \cdot e^{-\pi_M A_D / kT} \cdot e^{-\psi F z / RT}, \quad (10)$$

where F is the Faraday constant and z the charge of the molecule.

In the context of membrane permeation, the dimensionless lipid–water partition coefficient or mole fraction, γ_{lw} is generally used

$$\gamma_{lw} = C_m / C_{eq}, \quad (11)$$

where C_m is the concentration of drugs per liter lipid and C_{eq} the concentration of free drug in solution. The two partition coefficients, K_{lw} and γ_{lw}, are related as follows,

$$\gamma_{lw} = b \cdot K_{lw}, \quad (12)$$

where b has the dimension [mol/L]. If we assume for simplicity that one mole of lipid corresponds approximately to one liter of lipid, the factor is $b \approx 1$.

2.8. Estimation of permeability coefficient, P, and the flux, Φ_M

The permeability coefficient, P, is directly proportional to the product of the lipid–water partition coefficient, γ_{lw}, and the diffusion coefficient, D, of the drug and is inversely proportional to the thickness of the membrane, Δx,

$$P = \gamma_{lw} \cdot D / \Delta x. \quad (13)$$

The diffusion coefficient, D, is, in turn, inversely related to the radius, r, of the diffusing particle and the viscosity of the membrane, η,

$$D = kT / (6\pi\eta r). \quad (14)$$

We used the radius, r, of the cross-sectional area, A_D, of the compounds. The flux, Φ, is then defined as the product of the permeability coefficient, P (Eq. (13)), and the concentration gradient, ΔC, between the intracellular and extracellular environment. If only the initial external aqueous concentration, C, is taken into account the flux can be expressed as,

$$\Phi_M = C \cdot P. \quad (15)$$

In the case of charged compounds, it has to be considered that only the fraction of compounds which is uncharged can cross the lipid bilayer by passive diffusion as outlined in detail elsewhere [13].

2.9. Estimation of the mole fraction of substrates in the cytosolic membrane leaflet

The mole fraction of substrates, X_b, in the cytosolic membrane leaflet of inside–out membrane vesicles at the concentration of half-maximum activation, K_m, can be quantitatively estimated on the basis of the Michaelis–Menten equation as shown previously [19]

$$V_S = V_{max} \cdot C_S / (C_S + K_m). \quad (16)$$

The steady-state concentration of substrates in aqueous solution C_S can be approximated by the equilibrium concentration, C_{eq}, and can then be replaced by the quotient X_b/K_{lw} (Eq. (7))

$$V_S = V_{max} \cdot X_b / (X_b + K_m \cdot K_{lw}). \quad (17)$$

Half-maximum rate, $V_{max}/2$, is reached if the mole fraction X_b corresponds to the product $K_m \cdot K_{lw}$. The mole fraction X_b of drugs in the cytosolic membrane leaflet at the concentration of half-maximum activation can thus be estimated as

$$X_b = K_m \cdot K_{lw}. \quad (18)$$

For a given compound and a given membrane, the concentration of half-maximum activation, K_1 (Eq. (1)) and the concentration of half-maximum activation, K_m (Eq. (16)), are comparable. The mole fractions given below correspond to $X_b = K_1 \cdot K_{lw}$.

3. Results

3.1. ECAR in MDR1-transfected cells measured as a function of time

We monitored the metabolic rate of living *MDR1*-transfected mouse embryo fibroblasts (NIH-MDR1-G185) and the corresponding wild-type cells (NIH-3T3) by measuring the ECAR (μpH units) by means of a Cytosensor microphysiometer [25]. The ECAR is essentially due to the efflux of lactic acid produced as a waste product upon ATP synthesis via glycolysis [24]. The ECAR induced by drugs or detergents in NIH-MDR1-G185 cells directly corresponds to the rate of ATP hydrolysis upon Pgp ATPase activation [20,21]. Fig. 1A–C show the ECAR of *MDR1*-transfected (NIH-MDR1-G185) mouse embryo fibroblasts and the corresponding wild-type (NIH-3T3) cells measured as a function of time in cell culture medium. The first data points in Fig. 1A–C reflect the basal metabolic rate defined as 100%. The subsequent two data points correspond to the ECAR upon perfusion of cells with verapamil (Fig. 1A), Triton X-100 (Fig. 1B) and Tween 80 (Fig. 1C) applied at an initial concentration, $C = 10$ μM, to both NIH-MDR1-G185 and NIH-3T3 cells, respectively. The modulation of the drug- or detergent-induced ECAR was reported as percentage variation of the basal rate. After stimulation for 3 min, during which two data points were recorded, cells were re-perfused with drug- or detergent-free medium until basal ECAR values were reached again before a further stimulation cycle was started. As seen in Fig. 1A–C, significant changes were observed in *MDR1*-transfected cells due to Pgp stimulation, but not in wild-type cells at the concentration used. Higher concentrations of Triton X-100 and Tween 80 also induced a metabolic change in wild-type cells. The ECAR changes in *MDR1*-transfected cells induced by detergents and drugs could be inhibited by cyclosporin A as shown below (Fig. 4A–C). This further demonstrated that the ECAR changes were due to the activation of the Pgp ATPase.

Verapamil and Triton X-100 (Fig. 1A and B) induced a maximum ECAR of ~170% and ~160%, respectively, after 40 s. Upon re-perfusion with detergent-free medium, basal values were reached again after approximately 20 min for Verapamil and Triton X-100. Tween 80 (Fig. 1C) induced an ECAR of ~135% after 40 s; however, the maximum ECAR of ~145% was reached only after re-perfusion with detergent-free medium for ~20 min, and basal values were reached again after about 80 min. This suggests that the concentration of 10 μM was close to the concentration at which the maximum Pgp ATPase activity of Tween 80 was reached and the second binding site started to get occupied. Upon re-perfusion of cells with medium the

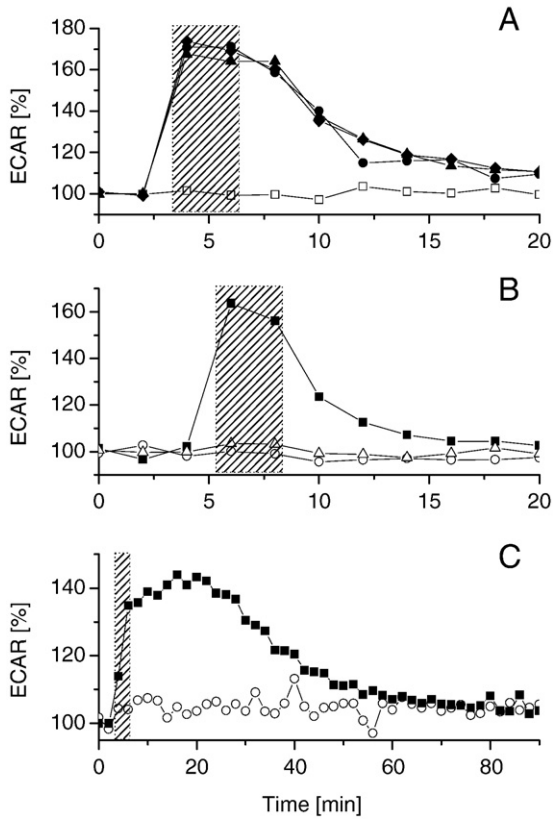

Fig. 1. (A–C) (A) Drug- and detergent-induced ECAR as a function of time. *MDR1*-transfected mouse embryo fibroblasts, NIH-MDR1-G185 (filled symbols), and wild-type mouse embryo fibroblasts, NIH-3T3 (open symbols). Stimulation by verapamil (A), Triton X-100 (B) and Tween 80 (C) each compound was applied at an initial concentration, $C = 10$ μM. Results are expressed as percent values of the basal ECAR taken as 100%. Hatched and cross-hatched areas indicate the stimulation period of 3 min. The different time scales should be noted. Data are average values of $n \approx 10$ experiments.

concentration of Tween 80 in the membrane, and concomitantly in the second, inhibitory binding site was diluted, leading to increased Pgp ATPase activity (for details, see Fig. 6 in ref. [21]). The relatively slow efflux times observed after re-perfusion of the cells with medium suggested that drugs and detergents are continuously flipped and leave the membrane only slowly.

3.2. ECAR of NIH-MDR1-G185 cells as a function of substrate concentration

As shown previously, the air–water partition coefficient, K_{aw}, of intrinsic Pgp substrates correlates reciprocally with the concentration of half-maximum Pgp ATPase activity, K_1 [32]. We therefore started the titration of the Pgp ATPase with drugs or detergents somewhat below the concentration, $1/K_{aw}$, of the compounds and ended it close to the critical micelle concentration, CMC (for data, see Table 1). Fig. 2A–C show the Pgp ATPase activity as a function of the concentration of the three drugs verapamil, diltiazem and daunorubicin in NIH-MDR1-G185 cells at pH7.4 and $T = 37$ °C. The ECAR was expressed as percent of the basal extracellular acidification rate taken as 100%. The data points correspond to the second stimulation point during the stimulation period of 3 min (see Fig. 1A–C) where a steady state was reached. We also measured the ATPase activity as a function of the drug concentration in inside–out plasma membrane vesicles made from NIH-MDR1-G185 cells by monitoring the phosphate release rate at pH 7.4 and $T = 37$ °C and data were included in Fig. 2A–C for comparison. The activity profiles obtained at pH 7.4 were very similar to those obtained previously at pH 7.0 [20].

Fig. 2D–F show the same data as Fig. 2A–C; however, expressed as drug-induced turnover number (i.e. after subtraction of the basal activity). It should be noted that the basal ECAR in cells reflects the total metabolism of the cell, including basal Pgp ATPase activity, whereas the basal phosphate release rate in inside–out plasma membrane vesicles reflects only the basal activity of the Pgp ATPase. The turnover number was calculated using a basal activity, $V_0 = 1.4 \times 10^7$ protons/cell/s and 1.95×10^6 Pgp molecules per cell [6]. Verapamil (Fig. 2A, D) and Diltiazem (Fig. 2B, E) enhanced the Pgp ATPase at low and reduced it at high concentrations, respectively, yielding bell-shaped activity profiles in inside–out vesicles and cells. Daunorubicin (Fig. 2C, F) inhibited the Pgp ATPase already at low concentrations in inside–out plasma membrane vesicles but activated it in cells.

Fig. 3A–F show the detergent-induced ATPase activity profiles in cells and inside–out membrane vesicles [22]. The two detergents $C_{12}EO_8$ and Triton X-100 (Fig. 3A, B) yielded bell-shaped activity profiles, comparable to those observed in inside–out plasma

Table 1
Parameters obtained from ATPase activity and surface activity measurements, respectively.

Parameter	Verapamil	Diltiazem	Daunorubicin	Triton X-100	C12EO8	Tween 80
pK_a	8.9 ΔpK_a 1.2 [18]	7.7 [43]	8.4 (basic)[35] 9.5 (acidic)	–	–	–
K_1 (P) [M]	9.5×10^{-7} [18]	8.04×10^{-6}	6.8×10^{-7}[a]	8.96×10^{-7}	9.24×10^{-7}	1.12×10^{-8}
K_2 (P) [M]	3.7×10^{-5} [18]	1.87×10^{-3}	6.27×10^{-5}	5.66×10^{-5}	1.76×10^{-5}	1.28×10^{-7}
V_1 (P) [%]	260 [18]	285	118	188	175	108
V_2 (P) [%]	83	0	45	37	39	78
K_1 (ECAR) [M]	5.0×10^{-7} [21]	3.5×10^{-6} [21]	8.69×10^{-5}[b]	3.00×10^{-6}	1.30×10^{-6}	4.50×10^{-5}
K_2 (ECAR) [M]	3.73×10^{-5} [21]	2.97×10^{-4} [21]	n. d.	3.00×10^{-4}	5.00×10^{-5}	n. d.
V_1 (ECAR) [%]	160 [21]	180 [21]	14	168	263	154
V_2 (ECAR) [%]	110 [21]	80 [21]	n. d. 70	1	76	n. d.
X_b at K_1 (vesicles, cytosolic leaflet)	1.33×10^{-4}	4.38×10^{-4}	1.59×10^{-5}	1.43×10^{-2}	3.57×10^{-2}	1.04×10^{-3}
K_{aw} [M^{-1}][d]	1.66×10^{5}[c]	2.69×10^{4}	5.89×10^{5}	3.34×10^{6}	7.30×10^{6}	1.30×10^{8}
CMC [M]	5.0×10^{-3}	1.0×10^{-2}	$0.6–3 \times 10^{-4}$	0.23×10^{-3}	0.095×10^{-3}	0.01×10^{-3}
A_D [$Å^2$]	82 [31]	70 [32]	106 [32]	73.2	71.9	99.3
K_{lw} (from K_{aw}) [M^{-1}][d]	4.20×10^{2}	1.63×10^{2}	2.59×10^{2}	1.60×10^{4}	3.87×10^{4}	9.29×10^{4}
D [$cm^2 s^{-1}$]	4.45×10^{-8}	4.81×10^{-8}	3.91×10^{-8}	4.7×10^{-8}	4.75×10^{-8}	4.04×10^{-8}
Φ at K_1 [molecules $s^{-1} cm^{-2}$]	7.13×10^{15}	2.54×10^{16}	7.5×10^{14}	8.37×10^{16}	1.98×10^{17}	5.06×10^{13}
Φ at K_1 [molecules $s^{-1} cm^{-2}$]	1.61×10^{9}	5.74×10^{9}	1.70×10^{8}	7.57×10^{10}	1.79×10^{11}	7.32×10^{8}

[a] For daunorubicin the concentration of half-maximum activity, K_1, in inside–out membrane vesicles could not be evaluated with high accuracy due to the low Pgp ATPase activity. The concentration of half-minimum activity, K_2, could however be well determined, and the ratio K_2/K_1 seems reasonable compared to that of the other compounds.
[b] ECAR data were reevaluated according to the present new insights and differ from the previously published values [21].
[c] Measured at pH 8.0.
[d] K_{aw} and K_{lw} were determined at $T = 25$ °C. As discussed previously, values at $T = 37$ °C are almost identical [22], all other constants were determined at 37 °C.

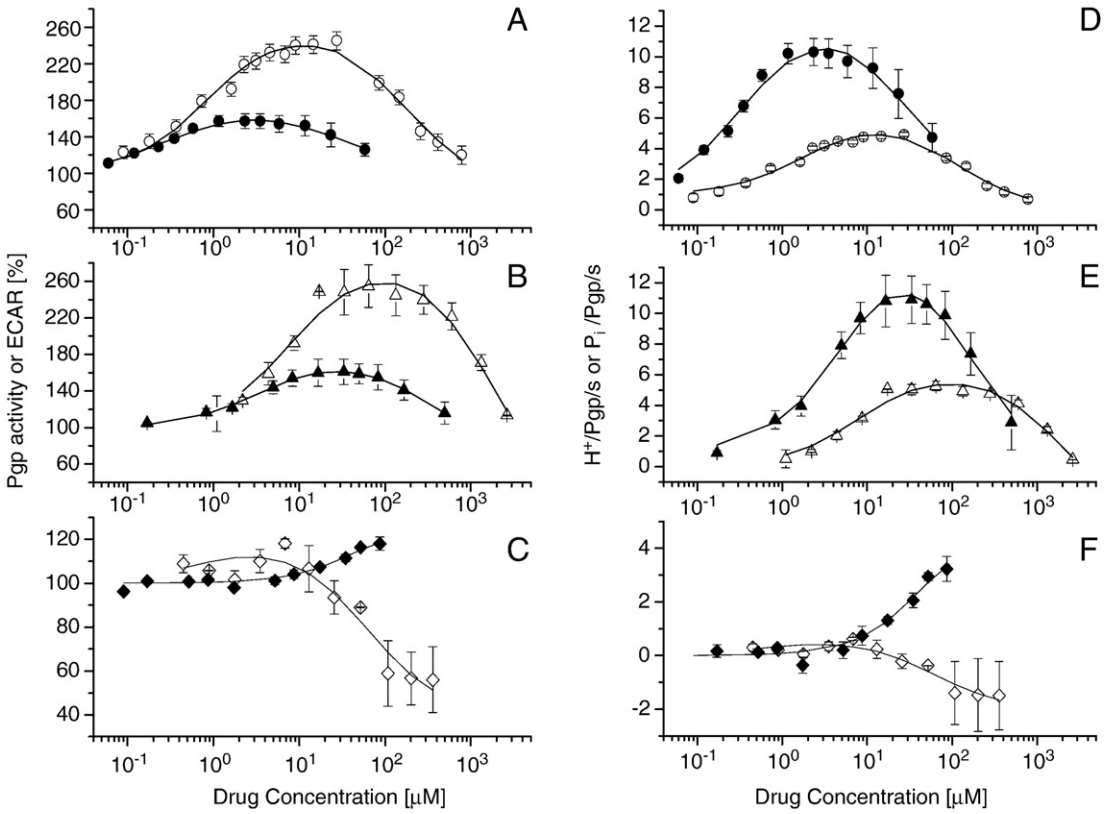

Fig. 2. (A–F) Pgp ATPase activity in NIH-MDR1-G185 cells (filled symbols) and inside–out plasma membrane vesicles (open symbols) induced by three drugs. (A–C) Pgp ATPase activity expressed as percent of the basal value in the absence of drugs. (D–F) Pgp ATPase activity expressed as protons (i.e. lactic acid) or phosphate released per Pgp per second. Calculations are based on the expression level of Pgp determined for NIH-MDR1-G185 by Ambudkar et al. [6]. (A, D) Verapamil (○, ●); B, E: diltiazem (△, ▲), and C, F: daunorubicin (□, ■). Lines are fits to Eq.(1). Standard deviations are shown.

membrane vesicles. However, Tween 80 (Fig. 2C) enhanced the Pgp ATPase activity in cells and inhibited it in inside–out membrane vesicles. The solid lines in Fig. 2A–F and Fig. 3A–F are fits to the modified Michaelis–Menten equation (Eq. (1)) [26], which is based on un-competitive or substrate inhibition [21]. The kinetic constants obtained from the fits are summarized in Table 1.

A closer look at the Pgp ATPase activity profiles induced by Triton X-100, C12EO8 and Tween 80 in inside-out plasma membrane vesicles (Fig. 3A, B, C) shows that the activating branch decreases in the order given. As shown previously the affinity from water to the transporter increases in the same order [22]. An analogous decrease in activity with increasing substrate affinity from water to the transporter was observed previously for a larger set of compounds (Fig. 7 in ref. [20]; and Fig. 10 in ref. [22]). It can be explained by the high propensity of compounds with a high binding affinity to the transporter to occupy both binding sites already at very low aqueous concentrations if added to inside–out vesicles. Reduced activity due to high binding to the transporter was also observed for daunorubicin (Fig. 2F). Interestingly, a similar daunorubicin ATPase activity profile was observed previously with Pgp reconstituted in *Escherichia coli* lipids [33] which seem to exhibit a comparably high binding affinity to daunorubicin as the lipids in the plasma membrane of NIH-MDR1-G185 cells.

3.3. Inhibition of the Pgp ATPase activity in MDR1-transfected cells by cyclosporin A

Fig. 4 displays the Triton X-100-induced Pgp ATPase activity in the presence of increasing concentrations of the Pgp inhibitor cyclosporin A (0 μM (Fig. 4A), 1 μM (Fig. 4B) and 10 μM (Fig. 4C)). It shows that the Triton X-100-induced activity (8 μM) could be completely inhibited with cyclosporin A in cells. Inhibition of Triton X-100-induced activity was previously also shown in inside–out plasma membrane vesicles [22]. The concentration required to inhibit the Triton X-100-induced Pgp ATPase activity in Fig. 4C was however about seven-fold higher in cells than in inside–out membrane vesicles [22].

3.4. Detergents applied above the critical micelle concentration in living cells

The detergent-induced ATPase activity profiles (Fig. 3) were measured well below the CMC, and the detergent-induced effects were fully reversible. Fig. 5 shows the response of NIH-3T3 and NIH-MDR1-G185 cells to a Triton X-100 concentration ($C = 0.3$ mM) slightly above the CMC (CMC = 0.23 mM) applied for the same period of time (3 min) as in the previous experiments below the CMC. Above the CMC, Triton X-100 lead to a rapid and irreversible ECAR decrease in both, wild-type and transfected cells which is due to cell lysis. The Pgp ATPase was thus not able to protect the cells from lysis by Triton X-100 applied above the CMC.

3.5. The air–water partition coefficient and the cross-sectional area of substrates

Drugs and detergents were characterized by means of surface activity measurements. The air–water partition coefficients, K_{aw}, of the cationic drugs were measured previously at pH 7.4 and pH 8.0 (see references in Table 1). The higher pH value was used to minimize charge repulsion effects for the determination of molecular cross-sectional areas. Here we measured the surface pressure, π, of the three

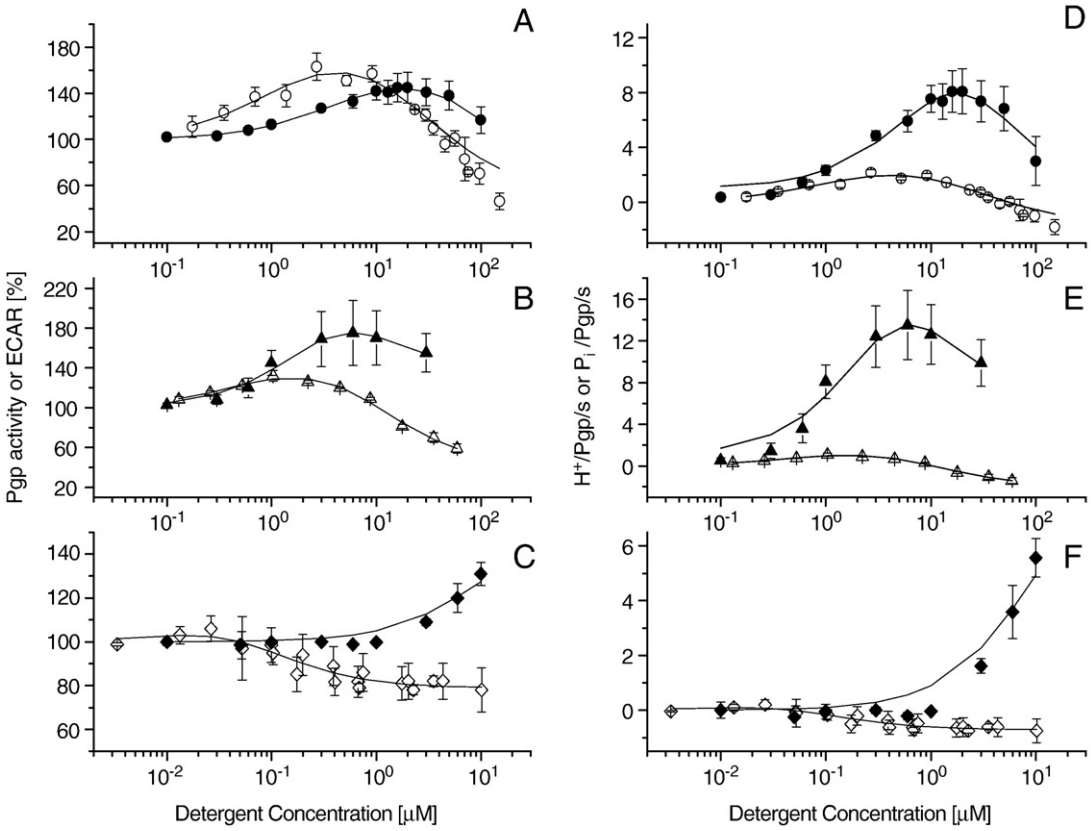

Fig. 3. (A–F) Pgp ATPase activity in NIH-MDR1-G185 cells (filled symbols) and inside–out plasma membrane vesicles (open symbols) induced by three detergents. (A–C) Pgp ATPase activity expressed as percent of the basal value in the absence of drugs. (D–F) Pgp ATPase activity expressed as protons (i.e. lactic acid) or phosphate released per Pgp per second. Calculations are based on the expression level of Pgp determined for NIH-MDR1-G185 by Ambudkar et al. [6]. (A, D) Triton X-100 (○, ●); (B, E) $C_{12}EO_8$ (△, ▲) and C, F: Tween 80 (□, ■). Lines are fits to the Eq.(1). Standard deviations are shown.

detergents as a function of time at different concentrations. The equilibrium surface pressure was reached after about 15 min in the case of Triton X-100 and $C_{12}EO_8$ and after more than 60 min in the case of Tween 80 (not shown) and was then plotted as a function of concentration (Gibbs adsorption isotherms). At low concentrations the surface pressure, π, increased slowly, then reached a constant slope up to the critical micelle concentration, CMC, from where the surface pressure increased no longer (not shown) (analogous measurements are described elsewhere in detail [29]). From the linear slope of the $\pi/\log C$ plot, the surface excess concentration, Γ_∞, (see Eq. (4)) and the cross-sectional area, A_D, of the molecule in its amphiphilic orientation at the air–water interface (see Eq. (3)) were derived. The air–water partition coefficient, K_{aw}, was then evaluated by fitting the data to Eq. (5). The cross-sectional area, A_D, of Triton X-100, $C_{12}EO_8$ and Tween 80 were determined as 73.2, 71.9 and 99.3 ^{2}, respectively, at pH 7.4. The data obtained from surface activity measurements are summarized in Table 1.

3.6. Estimation of the lipid–water partition coefficient of substrates

Knowledge of the cross-sectional area, A_D, and the air–water partition coefficient, K_{aw}, allows estimation of the lipid–water partition coefficient, K_{lw}, according to Eq. (9) for an electrically neutral membrane with a specific lateral packing density, π_M. For electrically neutral compounds and weak bases, an excellent prediction is obtained using the air–water partition coefficient, K_{aw}, determined at pH 7.4. For highly charged compounds such as verapamil, the prediction is better if the air–water partition coefficient, K_{aw}, is determined at pH 8.0 [29]. The lateral packing density of the plasma membrane of NIH-MDR1-G185 cells was previously estimated as $\pi_M = 30$ mN/m [21]. Lipid–water partition coefficients for drugs and detergents determined according to Eq. (9) are summarized in Table 1. The values are slightly higher than those measured for large unilamellar vesicles, LUVs, formed by 1-palmitoyl-2-oleoyl-*sn*-glycero-3-phosphocholine, POPC [22] exhibiting a lateral packing density of $\pi_M = 32$ mN/m [34].

NIH-MDR1-G185 cells and the corresponding inside–out plasma membrane vesicles showed a negative zeta potential in buffer solution containing magnesium chloride ($\zeta = -25$ mV) (see footnote 1 in Ref. [21]). In cells, the negative zeta potential arises from the glycocalix which may accumulate cationic drug in the vicinity of the electrically neutral lipid membrane surface. In inside–out vesicles, negative zeta potential arises from the negatively charged lipids in the cytosolic membrane leaflet. Provided the lipid asymmetry is

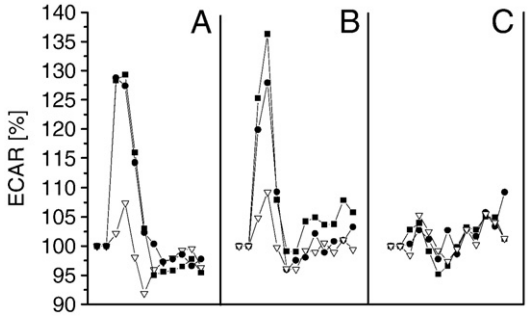

Fig. 4. (A–C) Inhibition of Triton X-100-induced ECAR by cyclosporin A. ECAR modulations in NIH-MDR1-G185 (●, ■) and NIH-3T3 (△) cells are shown, after 3 min exposure to 8 μM Triton X-100 alone (A), and in the presence of 1 μM (B) and 10 μM (C) cyclosporin A, respectively. The Triton X-100 and cyclosporin A concentrations were not corrected for adsorption.

maintained, a negative surface potential, $\psi = -30$ mV (related to the zeta potential), is adequate and yields lipid–water partition coefficients, K_{lw}, which are higher by maximally a factor of two for the three cationic drugs (not shown). For the following discussion, we assumed to a first approximation that the two plasma membrane leaflets exhibit the same lipid–water partition coefficients.

3.7. Estimation of permeability coefficient, P, and passive substrate influx, Φ_M

The permeability coefficient, P, and the flux, Φ_M, of drugs and detergents at their concentration of half-maximum activation, K_1, were calculated according to Eqs. (13) and (15) using the air–water partition coefficient, K_{aw}, and the cross-sectional area, A_D, determined by surface activity measurements (see Table 1), the lateral packing density of the mouse embryo plasma membrane, estimated as $\pi_M = 30$ mN/m [21], and a membrane viscosity, $\eta = 1$ poise. In the case of drugs, we took into account that only the fraction of uncharged drugs can permeate the membrane. The pK_a values used for calculations are included in Table 1 (for details see [13]).

The influx of verapamil, diltiazem and daunorubicin at the respective concentrations of half-maximum activation, K_1, was calculated as $\Phi_M \sim 7.13 \cdot 10^{15}$, $\Phi_M \sim 2.54 \cdot 10^{16}$ and $\Phi_M \sim 7.5 \cdot 10^{14}$ molecules$\cdot s^{-1} \cdot cm^{-2}$, respectively. For daunorubicin, experimentally determined values for the flux, Φ_M, across lipid bilayers are available [35], which allowed testing the present approach. Frézard and Garnier [35] measured the flux, Φ_M, of daunorubicin at a concentration, $C = 1$ μM across DNA-containing negatively charged lipid vesicles of different composition at pH 6.0 and a temperature, $T = 37$ °C. With a lipid mixture of phosphatidylcholine/phosphatidic acid/cholesterol (60/20/20), respectively, the flux was determined experimentally as approximately $\Phi_M \sim 2\ 10^{15}$ molecules s^{-1} cm^{-2}. Taking into account a negative surface potential of $\psi = -30$ mV and a lateral membrane packing density of $\pi_M = 30$ mN/m, we calculated the flux at pH 6.0 according to Eq. (13) as $\Phi_M \sim 1.5 \times 10^{14}$ molecules s^{-1} cm^{-2}. Considering that daunorubicin was dissolved in the presence of Triton X-100 (presumably to prevent self-association) which enhances permeation, and that the lipid/DNA ratio was most likely higher than in cells which may further enhance influx, the calculated value can thus be considered as reasonable estimate.

Permeability coefficients of the detergents calculated according to Eq. (13) are likely to be somewhat overestimated for the following reasons. Diffusion of the polyethoxylated and hydroxylated head groups may be more unfavorable than estimated on the basis of lipid–water partition coefficients. Upon insertion into a lipid layer the hydroxyl groups of detergents may remain fully or partially exposed to the aqueous phase, whereas upon diffusion or flip-flop the hydroxyl groups have to cross the hydrocarbon-like, hydrophobic core of the membrane. Comparing the partitioning of cyclohexane and cyclohexanol Wolfenden and Liang determined the standard free energy of transfer of a hydroxyl group (−OH), ΔG^0_{-OH}, from water to cyclohexane as $\Delta G^0_{-OH} = 23$ kJ/mol [36]. Using dodecyl methyl pentaerythrityl ethers, the standard free energy of transfer of a hydroxyl group from a less polar (hexane/chloroform) to the more polar phase (ethanol/water) was determined as $\Delta G^0_{-OH} = -559$ cal/mol (−2.24 kJ/mol) [37]. To estimate the influence of a hydroxyl group upon transfer of the detergent head groups to the hydrophobic core region of the membrane, the standard free energy of transfer ΔG^0_{-OH} was translated into a partition coefficient per hydroxyl group according to the following equation

$$\Delta G^0_{-OH} = -RT \ln K_{-OH}, \quad (19)$$

yielding a value of $K_{-OH} = 0.0001$ [36] and $K_{-OH} = 0.4$ [37]. The latter solvent mixtures seem to be more adequate to the present situation and therefore the permeability coefficients, P, (Eq. (13)) of detergents were multiplied by a factor of 0.4 per hydroxyl group. The flux of Triton X-100, $C_{12}EO_8$ and Tween 80 at the respective concentrations of half-maximum activation, K_1, was roughly estimated as $\Phi_M \sim 8.37 \times 10^{16}$, $\Phi_M \sim 1.98 \times 10^{17}$ and $\Phi_M \sim 5.06 \times 10^{13}$ molecules$\cdot s^{-1} \times cm^{-2}$, respectively. Considering the above discussion, the value given in Table 1 may be upper limits.

The cross-sectional area, A_D, of the molecule is a further parameter of relevance for passive influx. The area requirement of $C_{12}EO_n$ molecules ($n = 1$–8) in a liquid crystalline lipid bilayer was estimated previously by resonance energy transfer between the fluorescent probe molecules NBD-PE and rhodamine-PE [38]. For $C_{12}EO_8$ in a POPC bilayer, this yielded an area requirement of $A = 116$ Å^2 (see [38]). By X-ray diffraction, the cross-sectional area of $C_{12}EO_8$ was assessed as $A = 66$ Å^2, which is much closer to the value obtained from the Gibbs adsorption isotherm ($A_D = 71.9$ Å^2).

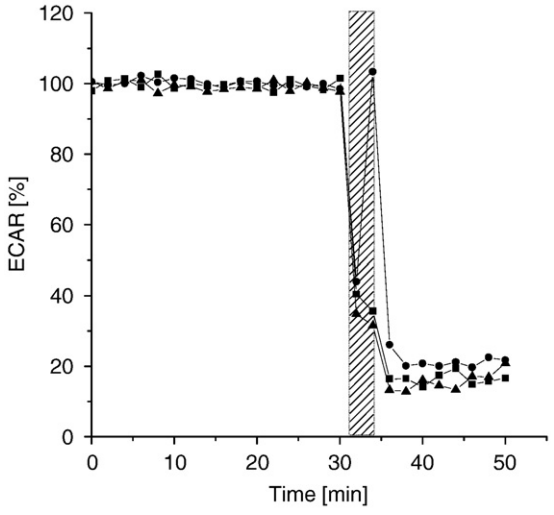

Fig. 5. Cell lysis upon addition of detergent above the CMC. Exposure of NIH-MDR1-G185 (■,●) and NIH-3T3 cells to 0.3 mM Triton X-100 during a period of 3 min (area outlined). ECAR modulations are expressed as percent of the basal value in the absence of drugs, which is arbitrarily defined as 100%.

4. Discussion

4.1. Substrate transport by Pgp

We measured the ATPase activity in NIH-MDR1-G185 cells and in the corresponding inside–out plasma membrane vesicles under steady-state conditions. Since the lipid bilayer of the plasma membrane highly accumulates the drugs [21], the processes observed, i.e. active substrate efflux by Pgp, V, and passive substrate influx, Φ_M, can be confined to the plasma membrane. The comparison of cells and inside–out plasma membrane vesicles can thus be considered as comparison of right side-out with inside–out plasma membranes as illustrated in Fig. 6, at least to a first approximation. Active efflux stands for the number of substrates moved from the cytosolic membrane leaflet to the extracellular leaflet per time and area, and passive influx stands for the number of molecules moved from the extracellular to the cytosolic membrane leaflet per time and area. Thereby, it has to be noted that active efflux is preceded by a diffusion step in cells but not in inside–out membrane vesicles. This difference is exploited to test the influence of diffusion on the ability of Pgp to protect the cells from intruding drugs and toxins. Calculations of passive influx across the lipid bilayer were used to verify data interpretation, but are not required per se to diagnose transport using ATPase assays as will be discussed in more detail below.

The two drugs verapamil and diltiazem (Fig. 2A, B, D, E) induced bell-shaped Pgp ATPase activity curves, in cells and inside–out plasma

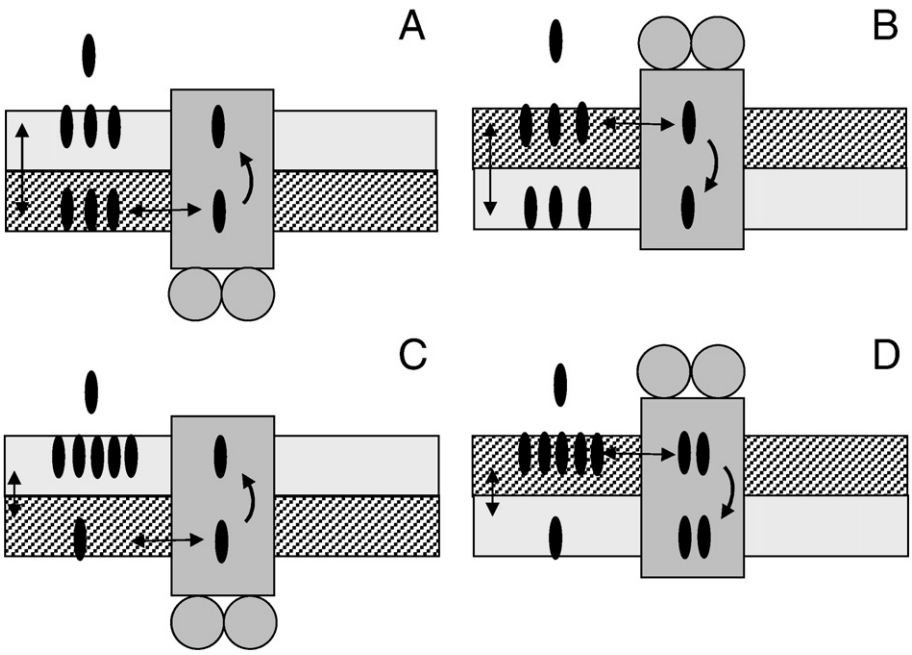

Fig. 6. (A–D) Drug access to the Pgp binding site in cells and inside–out vesicles. In cells, the drug has to diffuse across the lipid bilayer (A, C) to access the cytosolic membrane leaflet which harbors the substrate binding site of Pgp. In inside–out plasma membrane vesicles (B, D), it can directly access the cytosolic leaflet from the aqueous phase. The extracellular and the cytosolic membrane leaflets are indicated as gray and hatched, horizontal rectangles, respectively. Pgp is represented as vertical rectangle with two circles attached, representing the nucleotide binding domains. The black ovals indicate the compounds applied. (A and B) Compounds applied equilibrate rapidly (large arrow) between the two leaflets compared to efflux (smaller arrow). (C and D) Compounds equilibrate with similar rate compared to efflux (similar length of arrows). Under these conditions, Pgp is able to establish a concentration gradient.

membrane vesicles if applied as a function of concentration. The concentrations of half-maximum, K_1, and half-minimum, K_2, Pgp ATPase activity, respectively (see Table 1), were similar in the two systems suggesting that the mole fractions, X_b, of the two drugs in the cytosolic leaflet of cells and inside–out plasma membrane vesicles were also similar. The mole fraction, X_b, of drugs in the cytosolic membrane leaflet of inside–out membrane vesicles was estimated according to Eq. (18) (Table 1). This implies that the two drugs equilibrated rapidly between the cytosolic and extracellular leaflet of the plasma membrane in both systems. Passive influx of verapamil and diltiazem at their concentration of half-maximum activation, K_1, was determined as $\Phi_M = 1.61 \times 10^9$ molecules s^{-1} $cell^{-1}$ and $\Phi_M = 5.74 \times 10^9$ molecules s^{-1} $cell^{-1}$ respectively, which is indeed more than one order of magnitude higher than active efflux by Pgp determined previously as $V = 10^7$–10^8 molecules s^{-1} $cell^{-1}$ [20]. The situation of compounds equilibrating rapidly between the two membrane leaflets compared to the rate of transport by Pgp is illustrated schematically for cells (Fig. 6A) and inside–out membrane vesicles (Fig. 6B).

Titration of the Pgp ATPase with daunorubicin yielded in contrast significantly different activity profiles in cells and inside–out membrane vesicles (Fig. 2C, F). In cells, only the activating branch of the Pgp ATPase activity profile was observed ($K_1 = 8.69 \times 10^{-5}$ M), suggesting that the concentration (or mole fraction) of daunorubicin in the cytosolic membrane leaflet was relatively low and only one Pgp binding site was occupied by the drug. In inside–out plasma membrane vesicles, the inhibitory branch was predominant ($K_2 = 6.27 \times 10^{-5}$ M), suggesting that the concentration in the cytosolic membrane leaflet was significantly higher and both Pgp binding sites were occupied by daunorubicin.

The daunorubicin-induced concentration of half-maximum activity in inside–out membrane vesicles was determined as $K_1 = 6.8 \times 10^{-7}$ M. It seems reasonable to assume that the mole fraction in the cytosolic leaflet required to elicit a given response is identical in cells and inside–out membrane vesicles. The aqueous daunorubicin concentration required to elicit half-maximum activity in cells was much higher ($K_1 = 8.69 \times 10^{-5}$ M). Assuming identical binding constants for the two membrane leaflets and a linear increase with the aqueous concentration of daunorubicin, the mole fraction of daunorubicin in the extracellular leaflet of cells should be approximately two orders of magnitude higher (as derived from the ratio K_1 (cell) / K_1 (vesicle) = 127). This value may be somewhat overestimated since the increase in binding is no longer linear at high daunorubicin concentrations. For daunorubicin, the mole fraction ratio between the extracellular and the cytosolic leaflet in cells is therefore estimated as $X_b \leq 127$. The concentration gradient observed suggests that Pgp was able to cope with the low influx of daunorubicin ($\Phi_M = 1.7 \cdot 10^8$ molecules s^{-1} $cell^{-1}$). The situation of compounds equilibrating slowly between the two membrane leaflets compared to the rate of transport by Pgp is illustrated in Fig. 6C, D.

In the case of detergents, analogous observations were made. The more rapidly diffusing compounds Triton X-100 ($\Phi_M = 7.57 \times 10^{10}$ molecules s^{-1} $cell^{-1}$) and $C_{12}EO_8$ ($\Phi_M = 1.79 \times 10^{11}$ molecules s^{-1} $cell^{-1}$) induced similar bell-shaped Pgp ATPase activity profiles in inside–out membrane vesicles and cells, suggesting similar detergent concentrations in the cytosolic leaflet of the lipid membrane independent of the side of application. The small shift of the concentration of half-maximum activation, K_1, to higher values and the concomitant stronger activation in cells compared to inside–out membrane vesicles is due to a reduced concentration of detergents in the cytosolic leaflet, either because of a lower passive flux (see section 3.7) than given above or because of a slight absorption of detergents to the tubing of the Cytosensor.

The more slowly diffusing Tween 80 ($\Phi_M = 7.32 \times 10^8$ molecules s^{-1} $cell^{-1}$) showed only the activating branch of the activity profile in cells and a predominant inhibitory branch in inside–out membrane vesicles (Fig. 3C, D). For Tween 80, the mole fraction ratio between the extracellular and the cytosolic membrane leaflet was more than an

order of magnitude higher than for daunorubicin. This may be due to an even lower passive influx of Tween 80 than given in Table 1 (see section 3.7).

The analysis shows that high substrate concentrations in the extracellular leaflet of living cells (i.e. in the off-side of the Pgp ATPase) did not inhibit substrate unloading by Pgp as suggested previously based on experiments with inside–out membrane vesicles which exhibit a limited intra-vesicular space (see e.g. [11,39,40]).

4.2. Consequences for drug therapy

The present and previous [22] experiments revealed that it is relatively easy to reduce or inhibit the Pgp ATPase activity in inside–out membrane vesicles since molecules have direct access to the cytosolic leaflet membrane leaflet which harbors the Pgp binding site [12]. The most efficient inhibitors are hydrophobic compounds with a high lipid–water partition coefficient and/or compounds with a high affinity to the transporter in the lipid membrane [12,21] that occupy the second binding site of Pgp already at low aqueous concentrations. In excretory systems (liver and kidney), drugs or metabolites approach the apical membrane and Pgp from the basolateral side (i.e. from the same side as in inside–out plasma membrane vesicles). Pgp inhibition is thus facilitated and may contribute to cholestatic liver diseases.

In absorptive systems (blood–brain barrier, intestinal barrier and also in cancers), drugs or metabolites approach the apical membrane from the apical side. Binding to Pgp is therefore preceded by a passive diffusion step as in the cellular assay. The present experiments show that it is difficult to inhibit Pgp in cells because compounds bind to the extracellular membrane and reach the cytosolic membrane leaflet by passive diffusion across the lipid bilayer before binding to Pgp. Due to the "upstream" diffusion process Pgp gets the opportunity to cope with low substrate influx. Many Pgp inhibitors have low influx (i.e. a low product of the diffusion coefficient and concentration gradient) which reduces their concentration in the cytosolic membrane leaflet, prevents occupation of the second binding site of Pgp and in turn inhibition. It should be noted that in cells a ten times higher cyclosporin A concentration was required to inhibit Pgp (Fig. 4) than in inside–out vesicles [22]. The present results at least partially explain why Pgp inhibition in absorptive systems has so far not been as successful in clinical trials as expected on the basis of in vitro inhibition experiments [41].

As discussed elsewhere in detail [13], the active efflux, V, depends on the expression level of Pgp and only to a small extent on the lateral membrane packing density of the membrane [42]. Passive influx, in contrast, strongly (exponentially) depends on the lateral packing density of the membrane. It efficiently reduces passive influx which gives Pgp the chance to cope. Membranes with a high lateral packing density such as the BBB are therefore excellent barriers.

In summary, the different substrate pathways in living cells and inside–out plasma membrane vesicles to the Pgp binding site in the cytosolic membrane leaflet were exploited to monitor substrate transport by Pgp at the molecular level. The experiments revealed that export from the cytosolic leaflet back to the extracellular leaflet prevents substrate influx into the cytosol, provided that compounds diffuse slowly and do not disrupt the lipid bilayer. If influx of drugs or toxin is more than ten-fold higher than active efflux, the Pgp ATPase can no longer cope efficiently. Active efflux which is proportional to the rate of ATP hydrolysis varied by less than a factor of 10, whereas passive influx calculated at the concentration of half-maximum activity, K_1, varied by about three orders of magnitude for the different compounds. Passive influx is thus the dominant factor. If Pgp can cope with influx, a concentration gradient is established across the plasma membrane of cells (with a lower concentration in the cytosolic leaflet) which can be roughly quantified based on simple thermodynamic and kinetic principles. Whereas bi-directional transport assays reveal the net flux of compounds, measurement of substrate-induced P-glycoprotein ATPase activity in living *MDR1*-transfected cells and inside–out plasma membrane vesicles performed in parallel yields direct insights into substrate transport at the molecular level.

Acknowledgments

We are indebted to Dr. M.M. Gottesman and Dr. S. Ambudkar for providing the NIH-MDR1-G185 cells and the corresponding wild-type cells. P. Nervi is grateful for the opportunity to learn the handling of the cells in their laboratory. This work was supported by the Swiss National Science Foundation (Grant # 3100-107793).

References

[1] G. Szakacs, J.K. Paterson, J.A. Ludwig, C. Booth-Genthe, M.M. Gottesman, Targeting multidrug resistance in cancer, Nat. Rev. 5 (2006) 219–234.
[2] S. Dey, M. Ramachandra, I. Pastan, M.M. Gottesman, S.V. Ambudkar, Evidence for two nonidentical drug-interaction sites in the human P-glycoprotein, Proc. Natl. Acad. Sci. U. S. A. 94 (1997) 10594–10599.
[3] Y. Raviv, H.B. Pollard, E.P. Bruggemann, I. Pastan, M.M. Gottesman, Photosensitized labeling of a functional multidrug transporter in living drug-resistant tumor cells, J. Biol. Chem. 265 (1990) 3975–3980.
[4] C.F. Higgins, M.M. Gottesman, Is the multidrug transporter a flippase? Trends Biochem. Sci. 17 (1992) 18–21.
[5] I.L. Urbatsch, B. Sankaran, S. Bhagat, A.E. Senior, Both P-glycoprotein nucleotide-binding sites are catalytically active, J. Biol. Chem. 270 (1995) 26956–26961.
[6] S.V. Ambudkar, C.O. Cardarelli, I. Pashinsky, W.D. Stein, Relation between the turnover number for vinblastine transport and for vinblastine-stimulated ATP hydrolysis by human P-glycoprotein, J. Biol. Chem. 272 (1997) 21160–21166.
[7] A.B. Shapiro, V. Ling, Stoichiometry of coupling of rhodamine 123 transport to ATP hydrolysis by P-glycoprotein, Eur. J. Biochem. 254 (1998) 189–193.
[8] W.D. Stein, Kinetics of the P-glycoprotein, the multidrug transporter, Exp. Physiol. 83 (1998) 221–232.
[9] G.D. Eytan, R. Regev, G. Oren, Y.G. Assaraf, The role of passive transbilayer drug movement in multidrug resistance and its modulation, J. Biol. Chem. 271 (1996) 12897–12902.
[10] J.H. Hochman, M. Yamazaki, T. Ohe, J.H. Lin, Evaluation of drug interactions with P-glycoprotein in drug discovery: in vitro assessment of the potential for drug-drug interactions with P-glycoprotein, Curr. Drug. Metab. 3 (2002) 257–273.
[11] H. Omote, M.K. Al-Shawi, A novel electron paramagnetic resonance approach to determine the mechanism of drug transport by P-glycoprotein, J. Biol. Chem. 277 (2002) 45688–45694.
[12] A. Seelig, E. Gatlik-Landwojtowicz, Inhibitors of multidrug efflux transporters: their membrane and protein interactions, Mini. Rev. Med. Chem. 5 (2005) 135–151.
[13] A. Seelig, The role of size and charge for blood–brain barrier permeation of drugs and fatty acids, J. Mol. Neurosci. 33 (2007) 32–41.
[14] M. Horio, I. Pastan, M.M. Gottesman, J.S. Handler, Transepithelial transport of vinblastine by kidney-derived cell lines. Application of a new kinetic model to estimate in situ Km of the pump, Biochim. Biophys. Acta 1027 (1990) 116–122.
[15] J.W. Polli, S.A. Wring, J.E. Humphreys, L. Huang, J.B. Morgan, L.O. Webster, C.S. Serabjit-Singh, Rational use of in vitro P-glycoprotein assays in drug discovery, J. Pharmacol. Exp. Ther. 299 (2001) 620–628.
[16] D. Schwab, H. Fischer, A. Tabatabaei, S. Poli, J. Huwyler, Comparison of in vitro P-glycoprotein screening assays: recommendations for their use in drug discovery, J. Med. Chem. 46 (2003) 1716–1725.
[17] K.M. Mahar Doan, J.E. Humphreys, L.O. Webster, S.A. Wring, L.J. Shampine, C.J. Serabjit-Singh, K.K. Adkison, J.W. Polli, Passive permeability and P-glycoprotein-mediated efflux differentiate central nervous system (CNS) and non-CNS marketed drugs, J. Pharmacol. Exp. Ther. 303 (2002) 1029–1037.
[18] M. Meier, X.L. Blatter, A. Seelig, J. Seelig, Interaction of verapamil with lipid membranes and P-glycoprotein: connecting thermodynamics and membrane structure with functional activity, Biophys. J. 91 (2006) 2943–2955.
[19] A. Seelig, E. Landwojtowicz, H. Fischer, X. Li Blatter, Towards P-glycoprotein structure–activity relationships, in: v.d. Waterbeemd, Artursson Lennernäs (Eds.), Drug Bioavailability/Estimation of Solubility, Permeability and Absorption, Wiley/VCH, Weinheim, 2003, pp. 461–492.
[20] P. Aanismaa, A. Seelig, P-glycoprotein kinetics measured in plasma membrane vesicles and living cells, Biochemistry 46 (2007) 3394–3404.
[21] E. Gatlik-Landwojtowicz, P. Aanismaa, A. Seelig, Quantification and characterization of P-glycoprotein–substrate interactions, Biochemistry 45 (2006) 3020–3032.
[22] X. Li-Blatter, P. Nervi, A. Seelig, Detergents as intrinsic P-glycoprotein substrates and inhibitors, Biochim. Biophys. Acta 1788 (2009) 2335–2344.
[23] C.O. Cardarelli, I. Aksentijevich, I. Pastan, M.M. Gottesman, Differential effects of P-glycoprotein inhibitors on NIH3T3 cells transfected with wild-type (G185) or mutant (V185) multidrug transporters, Cancer Res. 55 (1995) 1086–1091.
[24] E. Gatlik-Landwojtowicz, P. Aanismaa, A. Seelig, The rate of P-glycoprotein activation depends on the metabolic state of the cell, Biochemistry 43 (2004) 14840–14851.

[25] H.M. McConnell, J.C. Owicki, J.W. Parce, D.L. Miller, G.T. Baxter, H.G. Wada, S. Pitchford, The cytosensor microphysiometer: biological applications of silicon technology, Science 257 (1992) 1906–1912.
[26] T. Litman, T. Zeuthen, T. Skovsgaard, W.D. Stein, Structure–activity relationships of P-glycoprotein interacting drugs: kinetic characterization of their effects on ATPase activity, Biochim. Biophys. Acta 1361 (1997) 159–168.
[27] M.K. Al-Shawi, M.K. Polar, H. Omote, R.A. Figler, Transition state analysis of the coupling of drug transport to ATP hydrolysis by P-glycoprotein, J. Biol. Chem. 278 (2003) 52629–52640.
[28] H. Fischer, Passive Diffusion and Active Transport Through Biological Membranes—Binding of Drugs to Transmembrane Receptors, Philosophisch-Naturwissenschaftlischen Fakultät, Universität Basel, Basel, 1998, p. 170.
[29] G. Gerebtzoff, X. Li-Blatter, H. Fischer, A. Frentzel, A. Seelig, Halogenation of drugs enhances membrane binding and permeation, Chembiochem 5 (2004) 676–684.
[30] H. Fischer, R. Gottschlich, A. Seelig, Blood–brain barrier permeation: molecular parameters governing passive diffusion, J. Membr. Biol. 165 (1998) 201–211.
[31] G. Gerebtzoff, A. Seelig, In silico prediction of blood–brain barrier permeation using the calculated molecular cross-sectional area as main parameter, J. Chem. Inf. Model. 46 (2006) 2638–2650.
[32] A. Seelig, E. Landwojtowicz, Structure–activity relationship of P-glycoprotein substrates and modifiers, Eur. J. Pharm. Sci. 12 (2000) 31–40.
[33] I.L. Urbatsch, A.E. Senior, Effects of lipids on ATPase activity of purified Chinese hamster P-glycoprotein, Arch. Biochem. Biophys. 316 (1995) 135–140.
[34] A. Seelig, Local anesthetics and pressure: a comparison of dibucaine binding to lipid monolayers and bilayers, Biochim. Biophys. Acta 899 (1987) 196–204.
[35] F. Frézard, A. Garnier-Suillerot, Permeability of lipid bilayer to anthracycline derivatives. Role of the bilayer composition and of the temperature, Biochim. Biophys. Acta 1389 (1998) 13–22.
[36] R. Wolfenden, Y.L. Liang, Influences of solvent on group transfer potentials and biochemical recognition of carbohydrates. Anomalous solvation of the anomeric hydroxyl group, J. Biol. Chem. 263 (1988) 8022–8026.
[37] J.S. Berry, Structure and partition coefficient. Synthesis and properties of dodecyl methyl pentaerythrityl ethers, J. Org. Chem. 25 (1960) 1272–1274.
[38] G. Lantzch, H. Binder, H. Heerklotz, M. Wendling, G. Klose, Surface areas and packing constraints in POPC C (12)EO (n) membranes. A time-resolved fluorescence study, Biophys. Chem. 58 (1996) 289–302.
[39] Z.E. Sauna, M.M. Smith, M. Muller, K.M. Kerr, S.V. Ambudkar, The mechanism of action of multidrug-resistance-linked P-glycoprotein, J. Bioenerg. Biomembr. 33 (2001) 481–491.
[40] Z.E. Sauna, M. Muller, X.H. Peng, S.V. Ambudkar, Importance of the conserved Walker B glutamate residues, 556 and 1201, for the completion of the catalytic cycle of ATP hydrolysis by human P-glycoprotein (ABCB1), Biochemistry 41 (2002) 13989–14000.
[41] S. Shukla, C.P. Wu, S.V. Ambudkar, Development of inhibitors of ATP-binding cassette drug transporters: present status and challenges, Expert Opin. Drug Metab. Toxicol. 4 (2008) 205–223.
[42] P. Aanismaa, E. Gatlik-Landwojtowicz, A. Seelig, P-glycoprotein senses its substrates and the lateral membrane packing density: consequences for the catalytic cycle, Biochemistry 47 (2008) 10197–10207.
[43] M.S. Reza, M.A. Quadir, S.S. Haider, Comparative evaluation of plastic, hydrophobic and hydrophilic polymers as matrices for controlled-release drug delivery, J. Pharm. Pharm. Sci. 6 (2003) 282–291.